J Appl Physiol 102: 1057–1064, 2007.
First published November 9, 2006; doi:10.1152/japplphysiol.00114.2006.

An estimate of fetal autonomic state by time-frequency analysis of fetal heart rate variability

Maya David,[1] Michael Hirsch,[2] Jacob Karin,[1] Eran Toledo,[1] and Solange Akselrod[1]

[1]*The Abramson Institute of Medical Physics, Sackler Faculty of Exact Sciences, Tel Aviv University, Tel Aviv; and* [2]*Helen Schneider Hospital for Women, Rabin Medical Center, Petach Tikva, Israel*

Submitted 30 January 2006; accepted in final form 30 October 2006

David M, Hirsch M, Karin J, Toledo E, Akselrod S. An estimate of fetal autonomic state by time-frequency analysis of fetal heart rate variability. *J Appl Physiol* 102: 1057–1064, 2007. First published November 9, 2006; doi:10.1152/japplphysiol.00114.2006.—In this study we present a noninvasive method that enables the investigation of the fetal heart rate (FHR) fluctuations. The objective was to design a quantitative measurement to assess the fetal autonomic nervous system and to investigate its development as a function of the gestational age. Our Medical Physics group has developed a complex algorithm for online beat-to-beat detection of the fetal ECG (FECG), extracted from the maternal abdominal ECG signal. We used our previously acquired FECG data, which includes noninvasive recordings of 200 maternal abdominal ECG signals. From these, we chose 35 cases of healthy pregnancies that we divided into three groups according to gestational age: *Group 1,* 23 ± 2 wk; *Group 2*, 32 ± 1 wk; and *Group 3*, 39 ± 1 wk. The FHR variability was analyzed by a time-frequency decomposition based on a continuous wavelet transform. We showed that, independent of the gestational age, most of the FHR power is concentrated in the very-low-frequency range (0.02–0.08 Hz) and in the low-frequency range (0.08–0.2 Hz). In addition, there is power in the high-frequency range that correlates with the frequency range of fetal respiratory motion (0.4–1.7 Hz). In the intermediate-frequency range (0.2–0.4 Hz), the power is significantly smaller. The changes in the average power spectrum in relation to gestation time were carefully and quantitatively examined. The results imply that there is a neural organization during the last trimester of the pregnancy, and the sympathovagal balance is reduced with the gestational age.

autonomic nervous system; wavelet transform

THE AUTONOMIC NERVOUS SYSTEM (ANS) activity can be considered as a landmark of brain function, reflecting the overall fetal central nervous system (CNS) regulatory ability (16). Investigation of ANS activity during fetal gestational development may be one of the only available techniques for understanding fetal brain maturation.

We believe that an estimate of fetal ANS development may be a good surrogate to express fetal CNS development. By definition, appropriate ANS control requires the CNS to be able to process and integrate afferent neural information and direct an appropriate efferent neural (autonomic) response. For fetal autonomic control to be effective, a certain level of maturation of both the afferent and efferent divisions of the CNS is required, as is innervation of the heart tissue. Furthermore, these nerves must be able to generate active neurotransmitters, and the effector organ must have suitable receptors that will enable it to react to these neurotransmitters. In addition, the sympathovagal neural activity must be synchronized and integrated by the sinus node to achieve the reciprocal effect of increasing or decreasing the fetal heart rate (FHR; Ref. 18). As a result, we would expect to see more efficient ANS modulation of the heart rate (HR) at relatively advanced stages of pregnancy.

Since the fetus is not accessible to direct measurements, fetal ANS development is far from being fully disclosed. Spectral analysis of the HR fluctuations provides a quantitative amplitude and estimate of the cardiac ANS activity. A study of the periodicities of these fluctuations enables a noninvasive study of both the sympathetic and parasympathetic branches of the ANS. Hence, one can observe all of the HR variability (HRV) frequency components by applying a frequency-domain approach (1, 2).

In a healthy adult at rest, the HR power spectrum is concentrated in two main areas: the low-frequency (LF) range (typically <0.15 Hz) and the high-frequency (HF) range. The HF range contains one main peak called the HF peak, which coincides with the respiratory frequency. Physiological and pharmacological tests indicate that the HF range reflects the activity of the parasympathetic branch of the ANS, while the LF range is affected by both the sympathetic and parasympathetic branches (1). In children and adults, there are also very long-term regulations, e.g., body temperature variability or cyclic hormonal modifications. These regulations are reflected in the very-low-frequency (VLF) range (typically <0.05 Hz). Unlike in adults, there is no clear evidence indicating how HR fluctuations relate to the ANS in the fetus.

According to Hirsch, Karin, and Akselrod (18), long-term variability defines the slow cycling effect of FHR over time. In terms of frequencies, the long-term variability is normally in the range of 2–6 cycles/min (i.e., <0.1 Hz), with an amplitude that might rise up to 25 beats/min. FHR accelerations are a type of long-term variability. These accelerations are expressed by an increase in FHR relative to the baseline and can typically be related to fetal movements (31).

Short-term variability reflects the beat-to-beat changes due to the interval differences between successive R waves in the ECG signal. As opposed to the long-term variability, there is no existing formulation regarding the frequency range of the short-term variability in the fetus. Nevertheless, we expect these fluctuations to have higher frequency components.

There are evidences for FHR modulation during periods of fetal breathing movements (FBM), which, as in adults, are

Address for reprint requests and other correspondence: S. Akselrod, Tel-Aviv Univ., The Abramson Center for Medical Physics, School of Physics and Astronomy, P.O. Box 39040, Tel Aviv 69978, Israel (e-mail: solange@post.tau.ac.il).

The costs of publication of this article were defrayed in part by the payment of page charges. The article must therefore be hereby marked "*advertisement*" in accordance with 18 U.S.C. Section 1734 solely to indicate this fact.

called respiratory sinus arrhythmia (RSA; Refs. 13, 15, 33). The typical frequency range for the FBM is between 30 and 90 breathing movements/min; therefore, fetal RSA is an example of short-term variability.

During pregnancy, as the gestational age advances, the correlation between fetal body movements and FHR increases. Near the end of pregnancy, the correlation becomes highly significant, and FHR accelerations are visible in parallel to the fetal body movements. As a result, the HR data for a mature fetus is typically used to identify fetal behavioral states. It is common to distinguish between the quiescent and active fetal states. In the quiescent state, fetal movements are nearly unobservable, and the associated FHR is very stable, having a narrow oscillation bandwidth. In more active states, the fetal movements are more frequent, and the FHR is characterized by a wider oscillation bandwidth and frequent accelerations (14, 25, 28, 34).

Research on premature neonates does not provide enough knowledge concerning the in utero fetal ANS, due to breathing and other physiological differences. Furthermore, there is evidence for prolonged ANS immaturity in premature neonates (27). The present study is focused on a "normal" ANS development. Hence, it is essential to examine the fetus in its natural environment.

In recent years, the creation of noninvasive methods, such as real-time ultrasound, has extended the basic knowledge about the human fetus. Ultrasound can provide information about fetal cardiac function, body movements, respiratory activity, and behavioral patterns, yet it provides no information on the maturation of neural processes. Additionally, being a mechanical estimate, the time-resolution of ultrasound is quite low, and more information is required to improve the ability to detect cardiovascular and particularly neural malfunction prenatally.

Traces of the fetal cardiac electrical signal can be identified by attaching electrodes to the maternal abdomen from the 16th wk of gestation (8). In the last two decades, our Medical Physics group developed a unique and complex algorithm for online fetal ECG (FECG) detection. The FECG is noninvasively obtained by extraction from the maternal abdominal ECG signal (3, 20) and allows for beat-to-beat detection of the fetal R waves (even if hidden behind the maternal QRS complex; Fig. 1). This enables us to produce a very accurate instantaneous FHR signal.

The algorithm has additional applications in addition to revealing fetal heartbeats. It allows one to examine the complete fetal ECG waveform, such as the QRS complex, its shape and duration, PQ and QT interval, as well as T wave shape. This enables one to explore fetal cardiac morphology. An additional potential application is the analysis of the ST segment, as was successfully carried out during childbirth by Noren, Mer-Wahlin, and colleagues (23, 26).

Our ability to create an accurate FHR signal enables us to investigate the FHR fluctuations. Furthermore, this algorithm for FHR detection provides reliable results, even for relatively early stages of pregnancy. Consequently, it is possible to examine the progress of these FHR fluctuations as a function of the gestational time and to obtain a quantitative estimate of the autonomic control development in the fetus.

A time-frequency approach is used to investigate these fluctuations. Standard spectrum analysis is effective only when the frequency components are estimated under steady-state conditions of a signal (Fig. 2). When the signal includes events that occur over short time periods (such as a sudden motion) or in cases where the frequency components change over time (such as at onset and offset of fetal breathing motions), a different type of spectral analysis is required, namely a time-frequency approach (6, 7).

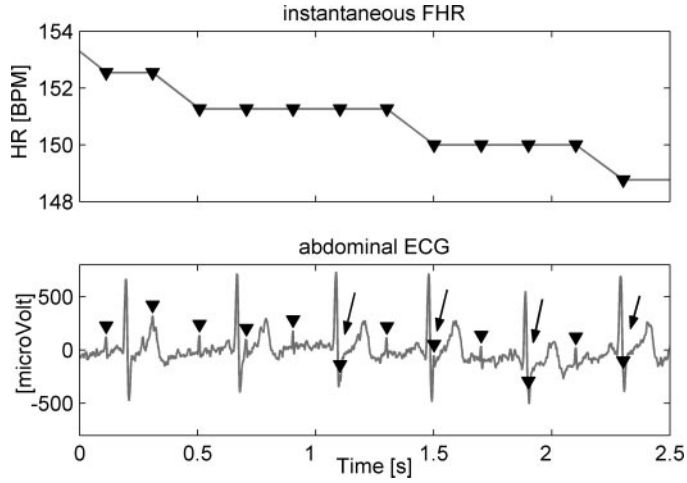

Fig. 1. Fetal R-wave detection. *Top*: instantaneous fetal heart rate (FHR); *Bottom*: abdominal ECG (▼ mark the fetal R waves). The arrows mark fetal R waves overlapping with maternal R waves. BPM, beats per minute.

The objectives of this work are to present noninvasive methods to assess the fetal ANS activity, to implement these new approaches to monitor the fetal periodical changes, and to estimate the fetal ANS maturation.

METHODS

Study Population

The study was approved by the Ethical Committee of Beilinson Medical Center. All subjects signed a written, informed consent form. In this work, we used abdominal ECG recordings acquired after completing the development of our FECG device. The abdominal ECG signals from 173 women were collected. This database includes recordings of both normal and abnormal pregnancies at different gestational ages.

Pregnancies with fetal cardiac malformations, fetal growth retardation, and maternal diabetes mellitus have been recorded ($n = 54$), and these cases were not included in our study. Twenty-one pregnancies close to labor, presenting maternal contractions, were also excluded from the analysis. Cases without known fetal or maternal pathology at the time of the ECG recording were considered as normal control ($n = 66$).

After careful sorting of the original database, 35 cases were selected from the group of normal pregnancies and further divided into three groups, according to their gestation period (Table 1). All 35 mothers did not smoke during the gestational period. There were no early births (average birth time: 39.5 ± 0.9 wk), and in all cases fetal weight at birth met the normal curve (average weight at birth: 3,370 ± 420 g).

We required that in each gestational age group the standard deviation would not exceed 2 wk from the average gestation age of the group. This rule was applied to eliminate the possibility that differences in the measured parameters would result from age differences within the groups.

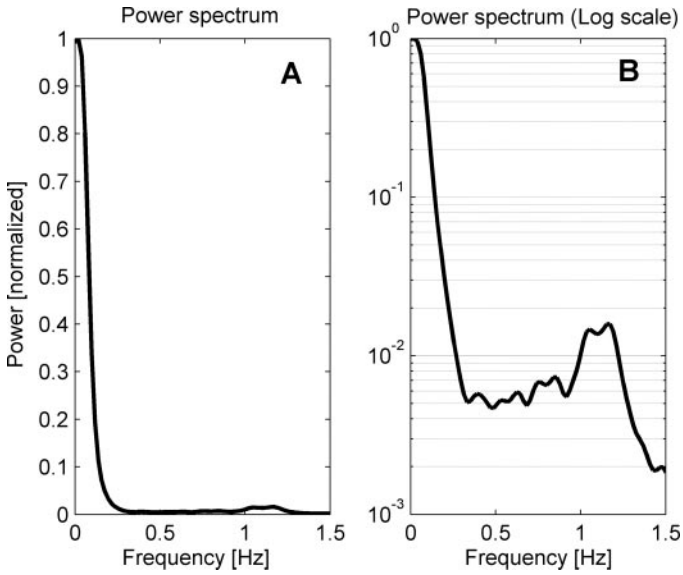

Fig. 2. Standard spectral analysis. *A*: power spectrum of FHR, 38 wk of gestation (GE). *B*: logarithmic scale emphasizes the weaker power in the higher frequencies range (>0.4 Hz) and displays the wide range of high frequencies (HF) compared with the stronger and narrower low-frequency (LF) range (<0.3 Hz).

Several cases deviated from the age ranges of the examined groups ($n = 16$), and additional age groups could not be constructed from them; therefore, we did not use their data.

In several additional cases ($n = 8$), the ECG recordings were shorter than 10 min, presenting larger statistical errors that would not allow a reliable analysis of the derived parameters. These cases were evaluated qualitatively, to ensure that there were no fundamental differences between these cases and the ones included in the study.

There are also restrictions regarding the application of spectral analysis: if the average FHR drops <130 beats/min, it could cause aliasing of the respiratory frequency, which is reflected in the FHR signal. The HR signal in fact performs a "sampling" of the respiratory motion cycles at the normal FHR (~2.4 Hz). As a result, when breathing is faster than one-half of the FHR (i.e., exceeds the Nyquist critical value ~1.2 Hz), it will cause aliasing (17). There were five cases where the average FHR dropped <130 beats/min. We also disqualified two cases (gestational ages: 33 and 40 wk), because their average FHR rose above 160 beats/min due to continuous accelerations. These active states are less representative [according to former observations, the fetus spends most of its time in less active states (31)]; however, their power values are very high and have a significant and decisive influence over the total power.

The original database also included 32 cases with insufficient quality of the abdominal ECG recording. In these cases, the algorithm did not succeed in identifying the fetal R waves for two key reasons: *1*) electrical interference (from external sources or as a result of strong maternal abdominal muscle activity); and *2*) attenuation of the intensity of the fetal R waves. This last reason is particularly common during 26–34 gestational weeks, possibly as a result of the fetal vernix covering its body almost completely, isolating the fetal cardiac electrical signal from the surrounding maternal tissue.

Data Acquisition

The recordings were conducted with the aid of a FECG and heart rate monitor (FEMO) system. This device was based on an algorithm developed by the Tel Aviv University Medical Physics group (20). The FEMO is a rapid computer-based noninvasive system that detects the superimposed maternal and fetal ECG signal from the mother's abdomen and then separates and processes the two signals independently. The application requires only a single lead with three electrodes and runs online on a personal computer with an analog-to-digital converter (sampling rate 300 Hz). For each case, an optimal signal-to-noise ratio determined the electrodes' configuration. During the development of the FEMO system, a validation procedure was performed by comparing with scalp ECG. In addition, during the processing procedure, a visual validation of the fetal QRS complexes detection was performed.

The FEMO allows for online beat-to-beat detection of the fetal R waves (Fig. 1). Every number in the R-R interval series corresponds to one fetal heartbeat, and, as a natural result, the intervals do not represent a uniform sampling of the tested process in the time domain. To perform a frequency domain analysis, the data must be sampled at regular time intervals; therefore, the R-R interval trace was resampled to produce a uniformly sampled HR signal (sampling rate 20 Hz; Ref. 4).

The Continuous Wavelet Transform for Time-Frequency Analysis of FHR

The continuous wavelet transform (CWT) maps the one-dimensional time-dependent signal into a two-dimensional frequency-time plane (9). We used a CWT to assess the time-dependent power spectrum of FHR fluctuations. This transform inherited the main features of the selective discrete Fourier transform algorithm (SDA), which was developed in our laboratory (21, 29). In the two transforms, the SDA and the CWT, the duration of the time frame is inversely proportional to the frequency of interest, i.e., $\Delta t \propto 1/f$.

As in all transformations between the time and frequency domains, Heisenberg's principle ($\Delta t \cdot \Delta f \geq 2\pi$) holds for the CWT. Thus, in our case, the frequency resolution is proportional to the frequency of interest: $\Delta f \propto f$.

These proportional relations indicate that the CWT has a high-frequency resolution (small Δf) along with a low time resolution (large Δt) in the LF range, and a low-frequency resolution with a high time resolution in the HF range.

An accurate selection of the LF and the HF ranges allowed the creation of dynamic parameters for the estimation of the fetal autonomic states. By integrating the CWT power density over the appropriate frequency bands, it is possible to examine the change of each relevant frequency band as a function of time.

Another dynamic parameter is the ratio between the LF band and the HF band, which might (as in adults) reflect the sympathovagal balance as a function of time (1, 5).

Statistics

One-way ANOVA, along with post hoc testing (Tukey), was applied for the comparisons between the groups' mean power values. Groups were considered as different when the P value was <0.05. When necessary, the power values have been modified (square root) to improve the normality of the distribution.

Table 1. *The three age groups*

	Number of Subjects	Mean Gestational Age, wk	Mean Duration of Abdominal ECG Recording, min
Group 1	10	23±2	13±2
Group 2	10	32±1	16±6
Group 3	15	39±1	24±10

Values are means ± SD.

RESULTS

Determining the General Features of a FHR Power Spectrum

We examined the results of the FHR spectral analysis for the entire data base (35 cases) and noticed a common denominator between the frequency components for these cases.

In Fig. 3, a typical FHR along with the corresponding time-frequency spectrum of the CWT is displayed. It is possible to observe a LF range (values that are <0.2 Hz) and a HF range (0.4–1.7 Hz). Between these two ranges, there is a sort of "gap" in which it is almost impossible to observe any power.

A similar pattern was observed repeatedly in all the cases we examined. There were no cases in which the HF and the LF merged (i.e., there were no cases without a gap). Therefore, we divided the frequency range into four sections: VLF (0.02–0.08 Hz), LF (0.08–0.2 Hz), intermediate (0.2–0.4 Hz), and HF (0.4–1.7 Hz).

Quantitative Results for Fetal Autonomic Development

We quantitatively examined the changes of the power spectrum according to the gestational age. For each frequency domain, the mean power values of the subjects as a function of the gestational age were displayed (Fig. 4, *A–C*).

VLF domain. VLF value was significantly different between the three age groups ($P = 0.007$). Analysis of the source of variance between these groups indicated that the value of VLF in *Group 1* was significantly lower than that in *Group 2*. The variance between *Group 3* and *Groups 1* or *2* was less pronounced.

LF domain. LF value was significantly different between the three groups ($P < 0.001$). Analysis of the source of variance between these groups indicated that the value of LF in *Group 1* was significantly lower than that in *Groups 2* and *3*. The variance between *Groups 2* and *3* was less significant.

HF domain. HF power was found to increase with gestational age ($P < 0.001$). The HF value in *Group 1* was significantly lower than that in *Groups 2* and *3*.

We also examined the VLF/LF, VLF/HF, and LF/HF ratios (Fig. 4, *D–F*).

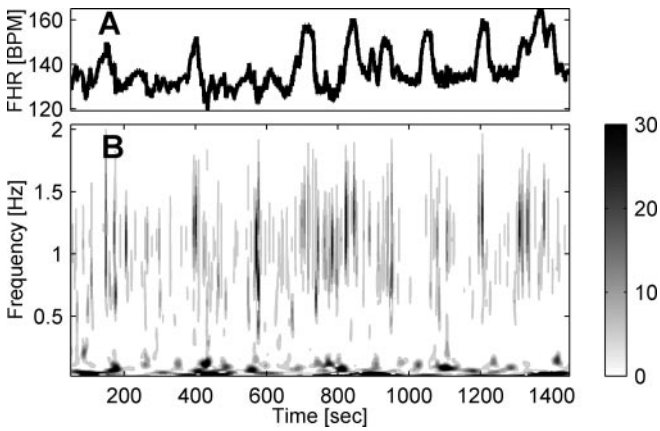

Fig. 3. Typical continuous wavelet transform (CWT) of FHR; GE: 38 wk. *A*: a very accurate FHR as a function of time (duration 1,400 s of recording), between 120 and 160 beats/min. *B*: CWT of FHR variability. The axes are: *x*-axis, time; *y*-axis, frequency; *z*-axis (grayscale), power density.

VLF/LF ratio. The VLF/LF ratio value was found to decrease with gestational age ($P < 0.001$). The VLF/LF ratio value in *Group 1* was significantly higher than that in *Groups 2* and *3*.

VLF/HF ratio. The VLF/HF ratio value was found to decrease with gestational age ($P = 0.007$). The VLF/HF ratio value in *Group 1* was significantly higher than in *Groups 2* and *3*.

LF/HF ratio. The difference between the three groups for the LF/HF ratio was not significant ($P = 0.4$).

Qualitative Examinations of the CWT Applications

We examined the applicability of CWT in two interesting cases to estimate whether the CWT can be an efficient tool for the investigation of FHR fluctuations.

Regular mouthing movements. According to descriptions in literature, Fig. 5*A* is a typical FHR pattern in case of fetal regular mouthing movements (gestational age: 38 wk; Refs. 10, 32). Figure 5*B* is the CWT of this FHR. Note the peak between 0.05 and 0.1 Hz in Fig. 5*B*. According to van Woerden et al. (32), this frequency peak matches the frequency observed during cases of fetal mouthing. We noticed similar results in two more cases (gestational age for both cases: 39 wk).

Periods of activity and quiescence. Figure 6*A* presents FHR patterns that correlate to active and quiescent fetal states. Analysis of the FHR data shows that the first time period represents an active state and the last period a quiescent state. In the LF range (Fig. 6, *B* and *D*), the FHR power spectrum values of the quiescent state are very low compared with those of the active state. In contrast, in the HF range (Fig. 6, *C* and *E*), there is no significant difference in the power values. Nevertheless, when the HF power distribution is examined, a clear difference between these two states of the HF range is observed. In the active state, the power is irregular (i.e., "smeared" over a wide HF range), whereas, during the quiet state, the power is much more regular (narrow HF range; see Fig. 6*C*).

DISCUSSION

The assessment of FHR variability (FHRV), especially when short-term variability is concerned, requires a very accurate detection of fetal heartbeats. There are only few available technologies that can achieve this required beat-to-beat accuracy; most of them are based on fetal magnetic heart signals (30, 33, 35).

The maternal abdominal ECG signal is a superposition of the cardiac electrical signal of the mother and the cardiac electrical signal of the fetus. Due to the indirect measurement and the differences in cardiac size, the fetal contribution is smaller by at least one order of magnitude. Furthermore, there are many additional noise sources, such as maternal muscle activity, uterine contractions, external electrical interference, etc. The FEMO algorithm overcomes these obstacles successfully and provides reliable and accurate results from the middle until the end of the pregnancy. This enabled us to explore the fetal autonomic development and maturation.

The large volume of research recently conducted in the field of HRV provides a precise description of the general features of the HR power spectrum in adults, which in turn allows one to investigate the ANS (1). Due to the lack of research in the

field of autonomic neural control in the fetus, there are still disagreements regarding the frequency ranges to be analyzed (VLF, LF, or HF) when investigating the FHRV. Applying the CWT algorithm for the time-dependent spectral analysis of the FHR provides a complete picture of the general features of the FHR fluctuations.

Three gestational age groups were examined (Table 1). In all the cases, the pattern was similar as far as frequency content

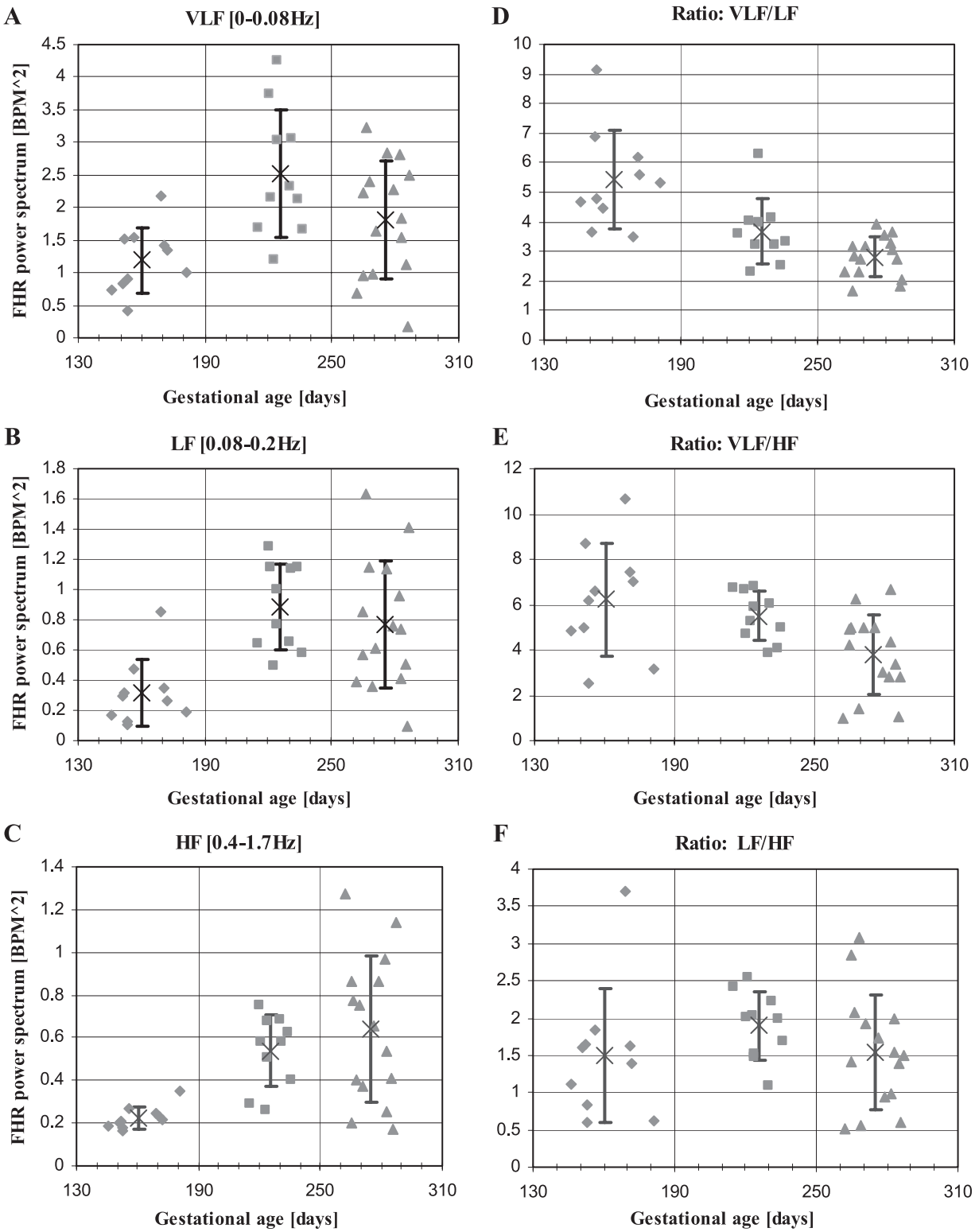

Fig. 4. Changes of the power with the gestational age. In all graphs (*A–F*), ◆ mark the values of the power for the 1st age group (middle of the 2nd trimester); ■ mark the 2nd age group (start of the 3rd trimester), and ▲ mark the 3rd age group (end of the 3rd trimester). For each group, we have indicated the average (marked as x) and its standard deviation.

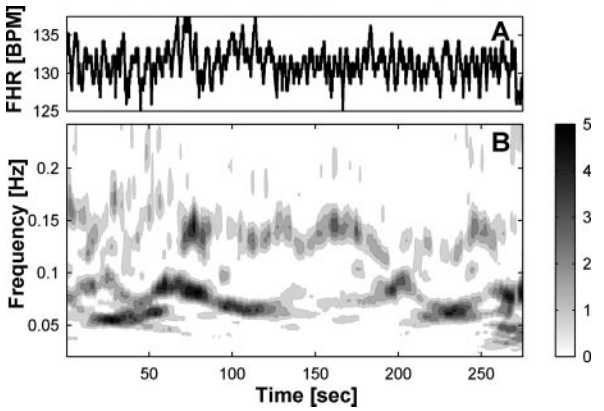

Fig. 5. FHR during fetal mouthing movements; GE: 38 wk. *A*: a typical FHR pattern of fetal mouthing (duration 250 s). *B*: CWT focus on the LF range. Notice the frequency between 0.05 and 0.1 Hz, which is typical for fetal mouthing.

was concerned (Fig. 3). We observed that most of the power is concentrated in the VLF range (0.02–0.08 Hz) and in the LF range (0.08–0.2 Hz). In addition, there is power in a wide HF range (0.4–1.7 Hz) that overlaps with the frequency range of the FBM. In the intermediate range (0.2–0.4 Hz), there is a significant drop in power of fluctuations (a kind of "power gap").

The CWT for Analyzing the FHR Fluctuations

In this study, we were interested in observing steady-state spectral components. Intuitively it would seem that standard spectral analysis could be sufficient for these conditions, but when monitoring fetuses, other factors, such as fetal motion, must be considered. The logarithmic display in Fig. 2 enables an intensification of the HF range, and it is obvious that in this range very little power is displayed spread over a wide range of frequencies (0.5–1.5 Hz). These frequency components obviously change in time.

Time-dependent spectrum analysis, on the other hand, allows for a more distinct understanding of the spectral components during dynamic (nonsteady) or active fetal states and their change over time.

We should mention that Kimura et al. (22) have also investigated the FHR fluctuations using wavelet transform. They focused on the LF range and demonstrated that the amplitude of temporal fluctuations of FHR has a gamma distribution.

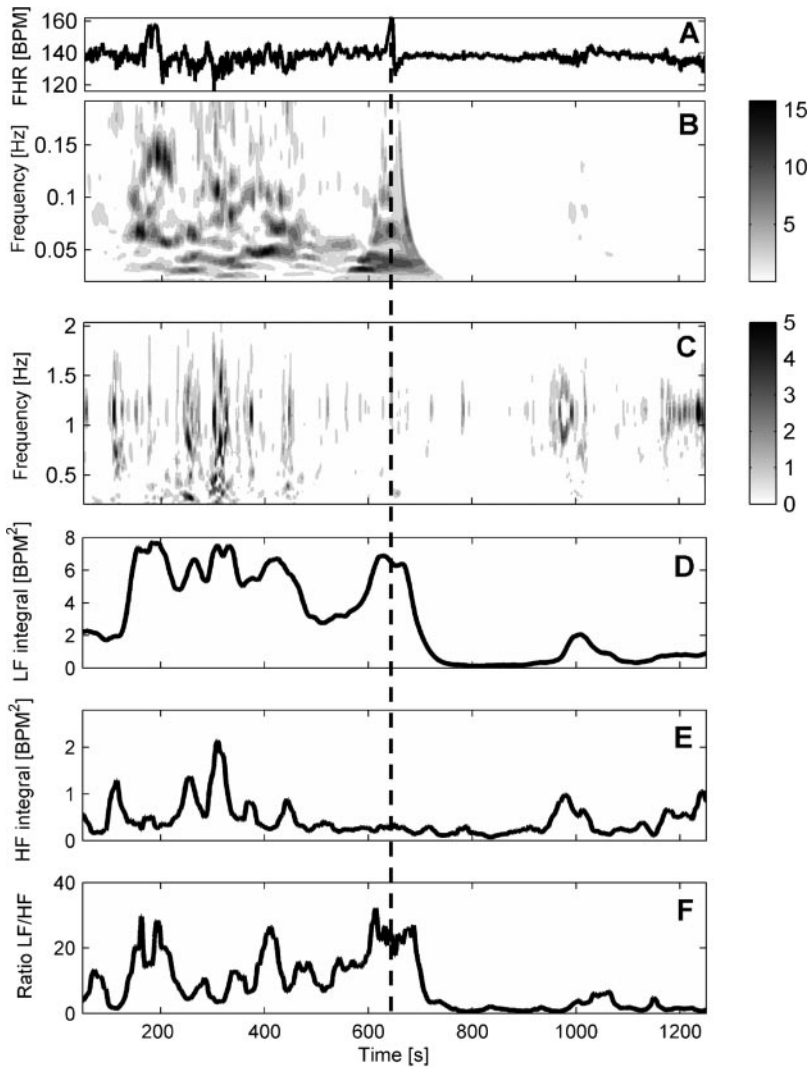

Fig. 6. Active state (*left*) compared with quiet state (*right*); GE: 38 wk. *A*: a typical FHR pattern that reflects active and quiet states. *B*: CWT, focus on the LF range. *C*: CWT, focus on the HF range. *D*: the power integral over the LF band. *E*: the power integral over the HF band. *F*: the sympathovagal ratio. All these graphs as a function of time, start during active state and change to quiet state around the dashed line.

The qualitative results proved that the CWT is an effective tool for the analysis of FHR fluctuations. The excellent frequency resolution in the VLF range allows the detection of frequencies related to fetal movements such as fetal mouthing activity (Fig. 5). The time-domain dependence of the CWT may assist in distinguishing between active and quiet states. In this regard, we presented a case where during active state the power was considerably higher than the power during quiet state (Fig. 6). We should emphasize that the qualitative results are examples that demonstrate the CWT's capability and possible further applications. At this stage, we do not intend to draw any specific conclusions regarding the physiological findings of these examples.

Power Spectrum Dependence on Gestational Age

The changes in the FHR power spectrum in relation to gestational age were examined quantitatively. Generally speaking, the power in *Group 2* increased significantly in relation to that in *Group 1*. However, the power differences between *groups 2* and *3* are less pronounced. A more specific analysis that takes the different frequency ranges into account provides details regarding the development of the ANS.

The HF average power was found to increase along with the gestational age (Fig. 4*C*). This result is not surprising, since there is evidence supporting an increase in the fetal breathing motion events and therefore in the occurrence of RSA, within the course of the pregnancy (33). In adults, the HF peak (at respiratory frequency) behaves as a measure of the parasympathetic activity, since the vagal system is modulated by respiration at the level of cardiac vagal motoneurons (16). Apparently, we can say that the fetal respiratory range (i.e., HF range) is an estimate of the fetal parasympathetic activity. However, the FBM is sporadic in time and irregular in frequency. A correct method to investigate the respiratory peak will therefore be to separate (based on the CWT) between FBM episodes and "apnea" and then to estimate the vagal tone.

The VLF range that coincides with the long-term variability is mostly affected by the FHR accelerations (11, 18). Therefore, the assumption that this frequency range reflects sympathetic activity seems reasonable. Figure 4*A* displays a significant power increase in *Group 2* compared with *Group 1*, and moderate power decrease in *Group 3* compared with *Group 2*. This result implies that there might be an increase in the sympathetic tone in the beginning of the third trimester (*Group 2*) and that this increase becomes more moderate during the last weeks of the pregnancy (*Group 3*), probably due to the appearance of fetal behavioral states (31).

The increase in FHR average power with gestational age in the LF range (Fig. 4*B*) resembles the VLF range power enhancement (Fig. 4*A*), i.e., in both cases the power increased significantly in *Group 2* compared with *Group 1* and then decreased moderately in *Group* 3 compared with *Group 2*. Furthermore, since the VLF/LF ratio (Fig. 4*D*) decreased significantly in *Group 2* compared with *Group 1*, we can conclude that the LF power increased more rapidly than the VLF power during the second half of the second trimester. This result implies that there might be a difference between the autonomic innervation related to the VLF and the autonomic branches related to the LF. Since the VLF range might be related to the sympathetic branch, we can assume that the LF range also has a vagal component, as observed in adult HRV analysis (1).

There was no significant difference between the three groups for the LF/HF ratio ($P = 0.4$). This result supports our previous conclusions, namely that both the LF and the HF have a vagal component, since the LF/HF ratio implies a similar behavior of these two power ranges.

Assuming that the VLF has a sympathetic component and that the LF has also a parasympathetic component, the ratio VLF/LF might reflect the sympathovagal balance. The results imply that there might be a gradual reduction in the sympathovagal balance during the last trimester.

As mentioned previously, we observed a power moderation starting around the beginning of the third trimester. A similar result was described by van Leeuwen et al. (30) and by Wakai (33), where magnetocardiogram recordings were used. This finding along with the appearance of fetal behavioral states implies that by the third trimester, the autonomic control has acquired a wide functioning range (possibly including an interaction between the sympathetic and parasympathetic system), and its average power values seem to become stabilized. Other studies that deal with fetal behavioral states reported that there is a behavioral organization during the last trimester (11, 12, 15, 19, 24). These observations imply that there might already be a basic organization of the nervous system starting around the 32nd wk of gestation.

In summary, the investigation of FHR fluctuations is essential, especially when dealing with the maturation of fetal cardiac autonomic control. The FEMO algorithm along with the CWT have proven to be sensitive tools that enable us to monitor the fetus in its natural surroundings. These techniques enable a noninvasive insight into the operational mode of the ANS.

REFERENCES

1. **Akselrod S.** Components of heart rate variability: basic studies. In: *Heart Rate Variability*, edited by Malik M and Camm AJ. Armonk, NY: Futura, 1995, p. 147–164.
2. **Akselrod S, Gordon D, Ubel FA, Shannon DC, Berger AC, Cohen RJ.** Power spectrum analysis of heart rate fluctuation: a quantitative probe of beat-to-beat cardiovascular control. *Science* 213: 220–222, 1981.
3. **Akselrod S, Karin J, Hirsch M.** Computerized detection of fetal ECG from maternal abdominal signal. *Comp Cardiol* 14: 261–264, 1987.
4. **Berger RD, Akselrod S, Gordon D, Cohen RJ.** An efficient algorithm for spectral analysis of heart rate variability. *IEEE Trans Biomed Eng* 33: 900–904, 1986.
5. **Bootsma M, Swenne CA, Van Bolhuis HH, Chang PC, Cats VM, Bruschke AV.** Heart rate and heart rate variability as indexes of sympathovagal balance. *Am J Physiol Heart Circ Physiol* 266: H1565–H1571, 1994.
6. **Challis RE, Kitney RI.** Biomedical signal processing (in four parts). Part 2. The frequency transforms and their inter-relationships. *Med Biol Eng Comput* 29: 1–17, 1991.
7. **Cohen L.** Time-frequency distributions—a review. *Proc IEEE* 77: 941–981, 1989.
8. **Curran JT.** *Fetal Heart Monitoring*. London: Butterworths, 1975.
9. **Daubechies I.** The wavelet transform, time-frequency localization and signal analysis. *IEEE Trans Info Theory* 36: 961–1005, 1990.
10. **de Vries J.** The first trimester. In: *Fetal Behaviour—Developmental and Perinatal Aspects*, edited by Nijhuis JG. Oxford: Oxford University Press, 1992, p. 3–11.
11. **DiPietro JA, Hodgson DM, Costigan KA, Hilton SC, Johnson TR.** Development of fetal movement—fetal heart rate coupling from 20 weeks through term. *Early Hum Dev* 44: 139–151, 1996.

12. **Dipietro JA, Irizarry RA, Costigan KA, Gurewitsch ED.** The psychophysiology of the maternal-fetal relationship. *Psychophysiology* 41: 510–520, 2004.
13. **Divon MY, Yeh SY, Zimmer EZ, Platt LD, Paldi E, Paul RH.** Respiratory sinus arrhythmia in the human fetus. *Am J Obstet Gynecol* 151: 425–428, 1985.
14. **Gagnon R, Campbell K, Hunse C, Patrick J.** Patterns of human fetal heart rate accelerations from 26 weeks to term. *Am J Obstet Gynecol* 157: 743–748, 1987.
15. **Groome LJ, Mooney DM, Bentz LS, Singh KP.** Spectral analysis of heart rate variability during quiet sleep in normal human fetuses between 36 and 40 weeks of gestation. *Early Hum Dev* 38: 1–9, 1994.
16. **Hainsworth R.** The control and physiological importance of heart rate. In: *Heart Rate Variability*, edited by Malik M and Camm AJ. Armonk, NY: Futura, 1995, p. 3–19.
17. **Hirsch M, Karin J, Shechter B, Segal O, Merlov P, Kaplan B, Akselrod S.** Detection of fetal breathing activity in real-time by means of spectral analysis of fetal heart rate fluctuations. *Proceedings of the 2nd World Congress of Perinatal Medicine, Rome, Italy, 19–24 September*, 1993, p. 535–539.
18. **Hirsch M, Karin J, Akselrod S.** Heart rate variability in the fetus. In: *Heart Rate Variability*, edited by Malik M and Camm AJ. Armonk, NY: Futura, 1995, p. 517–531.
19. **Karin J, Hirsch M, Akselrod S.** An estimate of fetal autonomic state by spectral analysis of fetal heart rate fluctuations. *Pediatr Res* 34: 134–138, 1993.
20. **Karin J, Hirsch M, Segal O, Akselrod S.** Noninvasive fetal ECG monitoring. *Comp Cardiol* 21: 365–368, 1994.
21. **Keselbrener L, Akselrod S.** Selective discrete Fourier transform algorithm for time-frequency analysis: method and application on simulated and cardiovascular signals. *IEEE Trans Biomed Eng* 43: 789–802, 1996.
22. **Kimura Y, Okamura K, Watanabe T, Yaegashi N, Uehara S, Yajima A.** Time-frequency analysis of fetal heartbeat fluctuation using wavelet transform. *Am J Physiol Heart Circ Physiol* 275: H1993–H1999, 1998.
23. **mer-Wahlin I, Hellsten C, Noren H, Hagberg H, Herbst A, Kjellmer I, Lilja H, Lindoff C, Mansson M, Martensson L, Olofsson P, Sundstrom A, Marsal K.** Cardiotocography only versus cardiotocography plus ST analysis of fetal electrocardiogram for intrapartum fetal monitoring: a Swedish randomised controlled trial. *Lancet* 358: 534–538, 2001.
24. **Nijhuis IJ, ten HJ, Nijhuis JG, Mulder EJ, Narayan H, Taylor DJ, Visser GH.** Temporal organization of fetal behavior from 24-weeks gestation onwards in normal and complicated pregnancies. *Dev Psychobiol* 34: 257–268, 1999.
25. **Nijhuis JG, Prechtl HF, Martin CB Jr, Bots RS.** Are there behavioural states in the human fetus? *Early Hum Dev* 6: 177–195, 1982.
26. **Noren H, mer-Wahlin I, Hagberg H, Herbst A, Kjellmer I, Marsal K, Olofsson P, Rosen KG.** Fetal electrocardiography in labor and neonatal outcome: data from the Swedish randomized controlled trial on intrapartum fetal monitoring. *Am J Obstet Gynecol* 188: 183–192, 2003.
27. **Patural H, Barthelemy JC, Pichot V, Mazzocchi C, Teyssier G, Damon G, Roche F.** Birth prematurity determines prolonged autonomic nervous system immaturity. *Clin Auton Res* 14: 391–395, 2004.
28. **Romanini C, Rizzo G.** Fetal behaviour in normal and compromised fetuses. An overview. *Early Hum Dev* 43: 117–131, 1995.
29. **Toledo E, Gurevitz O, Hod H, Eldar M, Akselrod S.** Wavelet analysis of instantaneous heart rate: a study of autonomic control during thrombolysis. *Am J Physiol Regul Integr Comp Physiol* 284: R1079–R1091, 2003.
30. **van Leeuwen P, Geue D, Lange S, Hatzmann W, Gronemeyer D.** Changes in the frequency power spectrum of fetal heart rate in the course of pregnancy. *Prenat Diagn* 23: 909–916, 2003.
31. **van Woerden EE, Van Geijn HP.** Heart rate patterns and fetal movements. In: *Fetal Behaviour—Developmental and Perinatal Aspects*, edited by Nijhuis JG. Oxford: Oxford University Press, 1992, p. 41–55.
32. **van Woerden EE, van Geijn HP, Caron FJ, Mantel R.** Spectral analysis of fetal heart rhythm in relation to fetal regular mouthing. *Int J Biomed Comput* 25: 253–260, 1990.
33. **Wakai RT.** Assessment of fetal neurodevelopment via fetal magnetocardiography. *Exp Neurol* 190*, Suppl* 1: S65–S71, 2004.
34. **Wheeler T, Murrills A.** Patterns of fetal heart rate during normal pregnancy. *Br J Obstet Gynaecol* 85: 18–27, 1978.
35. **Zhuravlev YE, Rassi D, Mishin AA, Emery SJ.** Dynamic analysis of beat-to-beat fetal heart rate variability recorded by SQUID magnetometer: quantification of sympatho-vagal balance. *Early Hum Dev* 66: 1–10, 2002.